

# Real-Time Spiking Neural Network: An Adaptive Cerebellar Model

Christian Boucheny<sup>1</sup>, Richard Carrillo<sup>2</sup>, Eduardo Ros<sup>2</sup>,  
and Olivier J.-M.D. Coenen<sup>1</sup>

<sup>1</sup> Sony Computer Science Laboratory Paris,  
75005 Paris, France

{boucheny, coenen}@csl.sony.fr

<sup>2</sup> Department of Computer Architecture and Technology,  
E.T.S.I. Informática, University of Granada,  
18071 Granada, Spain

{rcarrillo, eduardo}@atc.ugr.es

**Abstract.** A spiking neural network modeling the cerebellum is presented. The model, consisting of more than 2000 conductance-based neurons and more than 50 000 synapses, runs in real-time on a dual-processor computer. The model is implemented on an event-driven spiking neural network simulator with table-based conductance and voltage computations. The cerebellar model interacts every millisecond with a time-driven simulation of a simple environment in which adaptation experiments are setup. Learning is achieved in real-time using spike time dependent plasticity rules, which drive synaptic weight changes depending on the neurons activity and the timing in the spiking representation of an error signal. The cerebellar model is tested on learning to continuously predict a target position moving along periodical trajectories. This setup reproduces experiments with primates learning the smooth pursuit of visual targets on a screen. The model learns effectively and concurrently different target trajectories. This is true even though the spiking rate of the error representation is very low, reproducing physiological conditions. Hence, we present a complete physiologically relevant spiking cerebellar model that runs and learns in real-time in realistic conditions reproducing psychophysical experiments. This work was funded in part by the EC SpikeFORCE project (IST-2001-35271, [www.spikeforce.org](http://www.spikeforce.org)).

## 1 Introduction

Recently, an event-driven neural simulator has been devised that permits the simulation of thousands of conductance-based spiking neurons in real-time. The speed gain comes from precomputing into large lookup tables the differential equations governing neuron and synapse dynamics [1]. We demonstrate here how we used this simulator to run in real-time a realistic model of the cerebellum in a complete action-perception experimental setup. The model contains thousands of neurons and features a biologically plausible spike time dependent learning rule.

The cerebellar model is tested on learning in real-time to continuously predict the position of a target moving along periodical trajectories. This setup reproduces experiments with primates learning the smooth pursuit of visual targets on a screen [2]. When the eye is not on target, a retinal error signal is generated that drives neurons in the inferior olive of the cerebellum. These neurons activity directs plasticity in the cerebellum, hence modifying the eye movements to keep it on the visual target. Their low firing rate [3] is puzzling since it does not provide in one trial an accurate rendering of the retinal error. Nevertheless, a non-deterministic generation of spikes in these neurons is capable to sample, over multiple trials, the complete error range [4]. Hence, for the first time, a reliable performance in smooth pursuit is demonstrated with a complete model of the cerebellum with such a low firing rate encoding of the error.

The model and the architecture of the real-time simulating platform are presented in Sec. 2. The supervised learning mechanisms implemented in the network are explicit in Sec. 3. The performance of the model is shown in Sec. 4. The computational efficiency of the simulation framework allowed us to explore and demonstrate the stability of the learning mechanisms employed in the model over long periods of time.

## 2 Architecture of the Model

### 2.1 Cerebellar Network and Simulation Setup

The model described hereafter and shown in Fig. 1 reproduces the known anatomy of the cerebellum (see Ito [3] for a review).

The mossy fibers (MF) are the inputs to the model, carrying sensory information about the target: its lateral and longitudinal positions and velocities are encoded by 4 groups of 10 MF each. This information is transformed into a sparse representation in the large granule cell (GC) layer, in which each cell receives an excitatory connection from one randomly chosen neuron in each of the 4 MF groups. The granule cells then form with the Golgi cells (GO) an excitatory-inhibitory loop that limits the global activity in the granular layer.

The Purkinje cells, divided into 4 arrays of 4 neurons, receive excitatory inputs from all the GC axons, called parallel fibers (PF), and a connection from a single inferior olive (IO) neuron. The conductances of the PF-PC synapses are chosen randomly at the beginning of the simulation, and modified online during the learning of the task according to the rules defined in Sec. 3.

The output of the model is made of 4 cerebellar nucleus (CN) neurons, whose activity provides a prediction of future target position (the prediction is ahead by  $\tau_{pred}$ , set to 200 ms). Two neurons code for the predicted lateral position of the target  $X_{pred}$ , one for the ‘right’ position ( $Cn_{X_+}$ ), and the other for the ‘left’ position ( $Cn_{X_-}$ ). Similarly, the other two neurons code for the predicted longitudinal position  $Y_{pred}$ : ‘up’ ( $Cn_{Y_+}$ ) and ‘down’ ( $Cn_{Y_-}$ ). If  $Cn_i(t)$  is the activity of cell  $i$  at time  $t$ , computed from its spike train, the predicted position of the target at time  $t + \tau_{pred}$  is given by:

$$X_{pred}(t + \tau_{pred}) = Cn_{X_+}(t) - Cn_{X_-}(t) \quad (1)$$

$$Y_{pred}(t + \tau_{pred}) = Cn_{Y_+}(t) - Cn_{Y_-}(t) \quad (2)$$

Each CN neuron receives excitatory connections from all the mossy fibers, and inhibitory afferents from the 4 PCs of the same cluster (the PC-CN-IO subcircuit is organised in 4 microzones corresponding to the 4 variables coded by CN cells).

The inferior olive neurons carry the error signal that is used for the supervised learning of PF-PC synaptic conductances (see Sec. 2.2). Different sites of plasticity exist in the cerebellum [5], but the present model focuses on PF-PC plasticity, other synaptic conductances being fixed.

The spiking neurons of the network are simulated with a computationally efficient table-based event-driven simulator [1]. Such a paradigm is particularly suited for a cerebellar model in which sparse activity is expected in the numerous neurons of the granular layer [6]. Plasticity mechanisms have also been implemented in an event-driven scheme to permit online learning.

To close the sensorimotor loop, a time-driven simulation of the experimental setup was run in parallel (time step: 1 ms). It is used both to emulate the experimental world and to transform analog signals into spikes and vice-versa: conversion of sensory (target-related) and error signals into MF and IO spikes, and extraction of the target position prediction from CN spike trains.

As shown in Fig. 1, the two simulators communicate every millisecond through TCP/IP sockets that transmit buffered spikes.

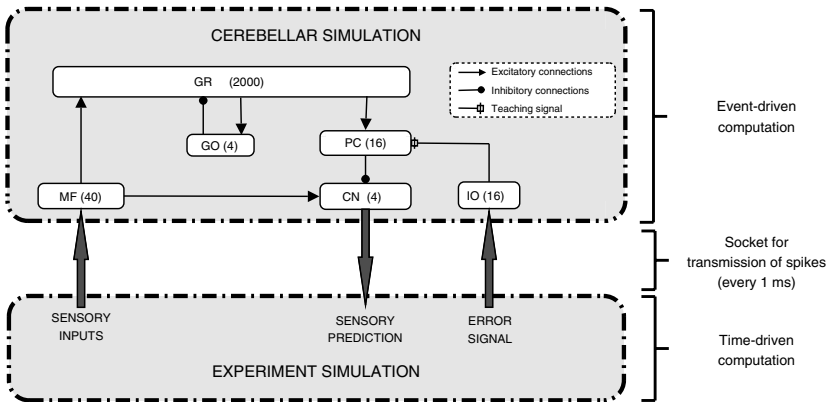


**Fig. 1.** Simulation set-up. The cerebellar model (top) described in Sec. 2.1 is run using an event-driven approach. It communicates through sockets with a time-driven simulator that emulates the experimental setup (movement of the target), generates the input spikes of the neural network and decodes cerebellar output spike trains. Numbers in parentheses in the cerebellar model diagram (top) represent the number of neurons per layer. MF: mossy fibers, GR: granule cells, GO: Golgi cells, PC: Purkinje cells, CN: cerebellar nucleus neurons, IO: inferior olive neurons

## 2.2 Models of Neurons

Mossy fibers are implemented as leaky integrate-and-fire neurons with the membrane potential  $U_m$  defined by the following equation [7]:

$$\tau_m \frac{dU_m}{dt} = -U_m(t) + RI(t) \quad (3)$$

When  $U_m$  reaches the threshold value  $U_{thresh}$ , the neuron fires and  $U_m$  is reset to the value  $U_{reset} < U_{thresh}$ . The input currents  $I(t)$  are computed by applying a radial basis function (RBF) to the coded sensory variable. The RBF centers are evenly distributed across the sensory dimensions, and their widths are chosen to ensure small response overlaps from consecutive mossy fibers.

The inferior olive neurons synapse onto the Purkinje cells and contribute to direct the plasticity of PF-PC synapses, which is believed to play a critical role in the learning of smooth and accurate movements [3]. These neurons, however, fire at very low rates (less than 10 Hz), which appears problematic to capture the high-frequency information of the error signal related to the task being learned. This apparent difficulty may be solved by their irregular firing, which can be exploited to statistically sample the entire range of the error signal over multiple trials [4]. This irregular firing is reproduced by means of a Poisson model of spike generation: if an IO neuron receives a normalised current  $I_{IO}(t)$  at time  $t$ , it will fire in the following time step if  $I_{IO}(t) > rand(t)$ , where  $rand(t)$  is a random number between 0 and 0.01 generated for the neuron at each time step (0.01 was chosen to limit the firing rate to 10 Hz).

Other cells are implemented as one-compartment conductance-based neurons, whose states are precomputed [1]. Parameters for the granule cells, Purkinje cells and Golgi cells were taken from electrophysiological recordings [1].

## 3 Learning

### 3.1 Plasticity Mechanisms

The main plasticity mechanism observed at the PF-PC synapse is long-term depression (LTD, i.e. a decrease in synaptic conductance) [3]. It is mainly triggered by the spikes of the IO cell contacting the corresponding PC, and depends upon past activity of the afferent PF. More precisely, a PF spike will induce more LTD if it occurs between 200 and 50 ms before the IO spike. To reproduce this, we implemented an ‘eligibility trace’ [2] for each plastic synapse by means of a kernel function  $K(t)$  applied to the spike train of the PF. The amplitude of LTD triggered by a IO spike at time  $t_{IO}$  is given by:  $\int_{-\infty}^{t_{IO}} K(t - t_{IO})\delta_i(t)dt$ , where  $\delta_i(t) = 1$  if the  $i^{th}$  PF fires at time  $t$ ,  $\delta_i(t) = 0$  otherwise. To fit the event-driven simulation framework, the kernel function was implemented as the weighted sum of three exponential functions with different time decays (Fig. 2).

Recent studies [8] have shown that cerebellar LTD can be reversed when PF spikes are followed neither by IO spikes nor by a strong depression of the PC

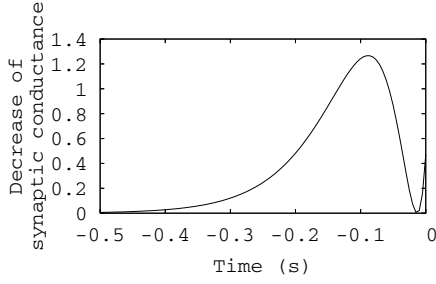


**Fig. 2.** Kernel used for PF-PC synaptic long-term depression. The kernel is convolved with the spike train of the afferent PF. This provides a measure of past PF activity setting the eligibility of the synapse to depression when the IO neuron afferent to the PC emits a spike ( $t = 0$ )

membrane potential. These findings were implemented by a non-associative plasticity rule: each time the presynaptic PF fires, the PF-PC synapse conductance is increased by a fixed amount  $\delta_{LTP}$ .

### 3.2 Generating the Error Signal

The input current driving the IO neuron is computed by comparing the predicted and the actual position of the target (prediction error). The error encoding by the inferior olive neurons follows the visual target position encoding by the CN neurons. To describe this error signal, let us consider the IO neuron  $i$  connected to a PC inhibiting the  $CN_{X_+}$  neuron (the one coding for prediction of positive lateral position of the target). Its input current at time  $t$ ,  $I(t)$ , is derived from the activity of  $CN_{X_+}$  at time  $t - \tau_{pred}$ , which represents the prediction for the positive lateral target position at time  $t$  ( $X_{pred+}(t) = CN_{X_+}(t - \tau_{pred})$ ), and from the actual lateral position of the target  $X_{target}(t)$ , according to the following equations:

$$\text{if } X_{target}(t) < 0, \quad I(t) = \alpha (0.15 - a X_{pred+}(t)) \quad (4)$$

$$\text{if } X_{target}(t) \geq 0, \quad I(t) = \alpha (0.15 + b (X_{target}(t) - X_{pred+}(t))) \quad (5)$$

where  $a$ ,  $b$  and  $\alpha$  are normalisation factors limiting the IO firing rate below 10 Hz (see Sec. 2.2). The value 0.15 was chosen to set the mean IO firing rate at 1.5 Hz for zero error, as observed experimentally.

The subtractive part of Eq. 4 represents formally the inhibition of the IO by CN neurons, which has been observed experimentally and suggested to be necessary for the reversal of non-relevant learning [9]. If the IO input current  $I(t)$  is close to 0, then LTP is likely to dominate LTD at the PF-PC synapse; if it is close to 1, then the contrary holds. The converse equations hold for the computation of the contralateral error (i.e. regarding  $CN_{X_-}$ ), and the same system of equations is used to generate the ‘up’ and ‘down’ error signals.

### 4 Experimental Task and Results

Psychophysical experiments have shown that monkeys can achieve accurate smooth pursuit eye tracking of periodically moving targets with hardly no phase lag, whereas delays in the visual pathway can reach over 100 ms. The flocculus and paraflocculus cerebellar areas participate to the control of smooth pursuit eye movements: they learn to produce movement predictions that compensate for the feedback delays in the eye control loop [2]. The present model is based on these findings and focuses on the ability of a cerebellar network to build short term predictions with physiologically constrained spiking learning mechanisms. A target moves along periodical trajectories and the model learns to build a continuous short-term prediction of the target position (Fig. 3, top right). At each time step, the cerebellar model is given the position and velocity of the target, and the CN neuron activities at time  $t$  are interpreted to compute the prediction of the target absolute position at time  $t + \tau_{pred}$  ( $\tau_{pred} = 200$  ms). The learning rules described in Sec. 3 are applied continuously.

The simulation consists of three consecutive stages of 1000 s. The target first describes an ‘8-shape’ trajectory with a period of  $2\pi$  s, then a circle with the

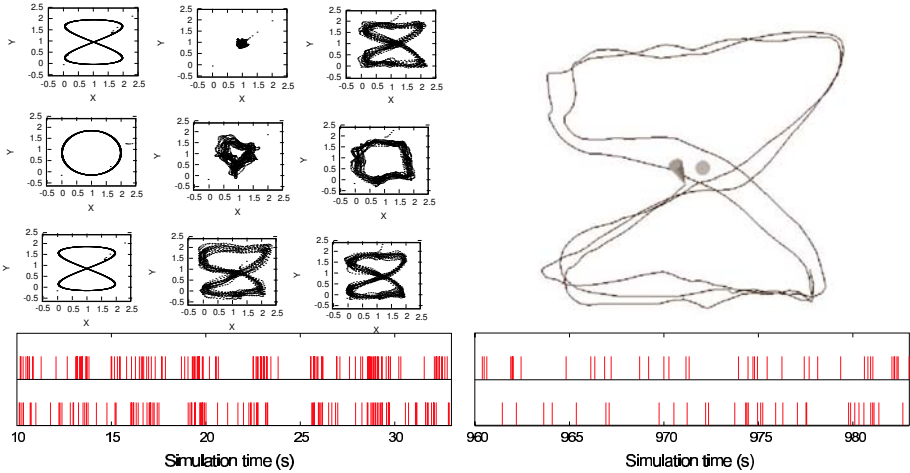


**Fig. 3.** Cerebellar model results. Top left: Performance of the model during three stages of 1000 s: ‘8-shape’ target trajectory (top), followed by a circle (middle) and finally an ‘8-shape’ again (bottom). The left column shows the target trajectories, the center and right columns represent, respectively, the predictions of the model at the beginning and the end of each stage. Top right: Screenshot taken at the end of the simulation. The target to follow is the ball, and the cone represents the delayed cerebellar sensory prediction. The lines are traces of past cerebellar output. Bottom: Spike trains of two IO cells coding for the same error signal, at the beginning of the simulation (left) and at the end of the simulation (right). When learning has stabilised, these cells fire at 1 to 2 Hz, whereas when the error is important frequencies up to 10 Hz can be observed

same period and finally the ‘8-shape’ trajectory again. This last stage seeks to test the possible destructive interferences brought by the second learning stage.

The performance of the model in the predictive task of smooth pursuit is illustrated in Fig. 3. The mean prediction error decreases from  $\eta = 0.6$  at the beginning of the simulation to  $\eta = 0.1$  after 3000 s. The spike trains of two IO cells related to  $CN_{X+}$  output neurons are also shown for the beginning and the end of the first stage of the simulation. The model learned to follow the given trajectory and little interference occurred when changing from one trajectory to another. Learning occurred mainly during the first 500 s of each stage and plateaued after this initial period. Indeed, the matrix of PF-PC weights remained stable afterwards, with only small local variations (not shown).

The simulations were run on a dual-processor computer (Intel(R) Xeon(TM) CPU 2.80 GHz). There were 2080 neurons in the network and more than 52000 synaptic connections. During one second of simulation, the cerebellar network received an average of 395 spikes, sent 405 spikes in output, and processed 935 801 events. One stage of the simulation (1000 s) lasted approximately 280 s, which revealed to be better than real-time. Hence, on this machine, there is room to scale up the size of the network, the main limiting factor being the global level of activity in the network.

## 5 Discussion

To our knowledge, the model presented here is the first to implement a complete and physiologically relevant spiking cerebellar network running in real-time and learning online to build sensory predictions in a closed sensorimotor loop. Good performances were reached despite the physiologically realistic low firing of the inferior olive (less than 10 Hz). This indeed suggests that one of the processing of the inferior olive is to sample non-deterministically the input signals it receives in order to provide over time a complete representation of these signals to the plasticity mechanisms at the Purkinje cells [4, 10]. The model extends many previous cerebellar models. Kettner et al. modeled the learning of predictive commands for smooth pursuit eye movements [2]. Their model featured an eligibility trace to compensate for visual feedback delays, but relied exclusively on analog units. Schweighofer et al. [11] and Spoelstra et al. [12] used the cerebellum to produce predictive corrections in an arm reaching task. Analog units were also used there, except for the IO cells modeled as leaky integrate and fire spiking neurons with low firing rates. However, the IO spikes were deterministically drawn from the error signal and the LTP at PF-PC synapse was modeled as a weights normalisation process. In a similar arm task, Kuroda et al. [4] showed that the stochastic firing of IO neurons increased performances; yet they implemented a very simplified cerebellar model and did not take time delays into account. In all the arm reaching simulations above, the learning took place per trial and not continuously and was implemented off-line, so that the output of the cerebellum could not interfere with the motor command during the learning stage. Medina et al. [13, 9] also implemented a spiking model of

the cerebellum, but they focused on eyeblink conditioning experiments and used coincidence-based learning rules.

Whereas with previous simulators hours or days were required to simulate a spiking cerebellar model learning smooth pursuit, the current event-driven simulator with online plasticity mechanisms permitted to achieve real-time learning of the task. This allowed us to show that the biologically plausible learning mechanisms running continuously over long periods of time were stable and that few destructive interferences occurred in learning the same task in different sensorimotor contexts (different target trajectories). Future simulation results will permit a thorough analysis of this evidence with more diverse contexts.

The current simulation framework demonstrates that a realistic spiking cerebellar model running in real-time in a complete action-perception sensorimotor loop is becoming reality. Future robotic experiments will sustain that claim.

## References

1. Carrillo, R.R., Ros, E., Ortigosa, E.M., Barbour, B., Agís, R.: Lookup Table Powered Neural Event-Driven Simulator. In: Proc. of the Eighth Int. Work-Conf. on Artif. Neural Networks, Springer-Verlag, LNCS series (2005)
2. Kettner, R.E., Mahamud, S., Leung, H., Sittkoff, N., Houk, J.C., Peterson, B.W., Barto, A.G.: Prediction of complex two-dimensional trajectories by a cerebellar model of smooth pursuit eye movement. *Journal of Neurophysiology* **77**(4) (1997) 2115–2130
3. Ito, M.: Cerebellar long-term depression: characterization, signal transduction, and functional roles. *Physiological Reviews* **81**(3) (2001) 1143–1195
4. Kuroda, S., Yamamoto, K., Miyamoto, H., Doya, K., Kawato, M.: Statistical characteristics of climbing fiber spikes necessary for efficient cerebellar learning. *Biological Cybernetics* **84** (2001) 183–192
5. Hansel, C., Linden, D.J., D’Angelo, E.: Beyond parallel fiber LTD: the diversity of synaptic and non-synaptic plasticity in the cerebellum. *Nature Neuroscience* **4**(5) (2001) 467–475
6. Coenen, O.J.M.D., Arnold, M.P., Sejnowski, T.J., Jabri, M.A.: Parallel fiber coding in the cerebellum for life-long learning. *Autonomous Robots* **11**(3) (2001) 291–297
7. Gerstner, W., Kistler, W.M.: Spiking neuron models. Cambridge University Press (2002)
8. Lev-Ram, V., Mehta, S.B., Kleinfeld, D., Tsien, R.Y.: Reversing cerebellar long-term depression. *Proceedings of the National Academy of Sciences* **100**(26) (2003) 15989–15993
9. Medina, J.F., Nores, W.L., Mauk, M.D.: Inhibition of climbing fibres is a signal for the extinction of conditioned eyelid responses. *Nature* **416** (2003) 330–333
10. Schweighofer, N., Doya, K., Fukai, H., Chiron, J.V., Furukawa, T., Kawato, M.: Chaos may enhance information transmission in the inferior olive. *Proceedings of the National Academy of Sciences* **101** (2004) 4655–4660
11. Schweighofer, N., Arbib, A.A., Kawato, M.: Role of the cerebellum in reaching movements in humans. II. A neural model of the intermediate cerebellum. *European Journal Of Neuroscience* **10** (1998) 95–105

12. Spoelstra, J., Schweighofer, N., Arbib, M.A.: Cerebellar learning of accurate predictive control for fast-reaching movements. *Biological Cybernetics* **82** (2000) 321–333
13. Medina, J.F., Mauk, M.D.: Simulations of cerebellar motor learning: computational analysis of plasticity at the mossy fiber to deep nucleus synapse. *The Journal of Neuroscience* **19(16)** (1999) 7140–7151